Enhanced Airfoil Design: LERC and TERC as MSBC Device on NACA 2412 Airfoil

Karan Shory[1], Harshdeep Singh[1], Sanjeev Kumar Dhama[1]
[1]*Department of Aerospace Engineering, Chandigarh University, 140413, Chandigarh, India*

***Abstract*—Based on the ideology of moving surface boundary layer control (MSBC), a rotating surface at the leading edge and trailing edge of an airfoil, tends to increase the aerodynamic efficiency of the airfoil. Hence, the given paper aims to design an optimal airfoil, which result in a better lift generation and delayed boundary layer separation. Implementation of rotating cylinder at leading edge (LERC) and trailing edge (TERC) is the key change in the geometry of conventional NACA 2412. Computational analysis described the design to be an augmentation to the major aerodynamic characteristic, i.e. lift generation. The comparison was made with pre-existing data from experimentation and computational analysis available in literature. Geometry has been proven to be of competence with the given diameters (D, and d) of LERC and TERC, and with given angular velocity, ω. The velocity relation proposed by MSBC has also been proven to be correct by simulated analysis. Conclusively, an ideal design has been drawn comprising of rotating edge on leading edge and trailing edge, which evidently performs better than conventional airfoils.**

Keywords*— *Moving Surface Boundary Layer Control (MSBC), Rotating Cylinder, Aerodynamic Efficiency, Lift Generation, Computational Analysis

I. INTRODUCTION

Since the idea of boundary layer has been introduced by Prandtl[1] in the early 20th century, aerodynamicists have been trying to use it to their advantage and develop a better lifting devices or configuration. A simple airfoil with high speed flow, may produce a boundary layer around it, consequently increasing the drag to a greater extent. The quest of optimizing the above said issues have lead to experiment with the boundary layer dynamics. The moving surface boundary layer control (MSBC) has been an approach with highest potential, as per the results available in literature[2,3,4]. In particular, implementation of rotating cylinders is the simplest and well published MSBC approach, which achieves the tasks with simplest geometrical design.

Moving surface boundary layer control (MSBC) involves to change the dynamic characteristics of a surface in order to change the boundary layer behaviour. Unlike static surfaces, the dynamic behaviour of the surfaces reacts with the fluid to achieve required outcomes. The motion of surface can be of various types, including oscillations, vibrations, rotation or translation. Sanjay's paper[5] on flow past rotating cylinder shows the effect of Magnus effect. The rotating cylinder experiences different drag and lift forces due to Magnus effect. This re-energizes the flow behind cylinder by controlling the boundary layer. These advantages of lift generation, delayed flow separation and enhanced control can be utilized to create a high lift device.

This idea of integrating the Magnus effect in the wing is already studied by various researchers[6,7,8]. Jonathan[9] studied the performance of airfoil in the wake of a circular spinning cylinder. The wake interference of the cylinder-airfoil alters airfoil performance for all x/D values. The circular motion imparted to the flow curves the flow over the airfoil which is at high angle of attack. This delays the flow separation; however, the flow must curve such that it attaches to the airfoil. This study shows how interaction of airfoil and cylinder can alter the aerodynamic performance. If used efficiently, it can delay flow separation and delay stall characteristics. Furthermore, Zhang[10,11] studied the interaction between wake of a airfoil and a rotating cylinder placed behind the airfoil. It is found that existence of upstream airfoil has a significant impact upon the flow drag and the lift produced by cylinder. For different Reynold's number, the vortices shed from the upstream airfoil lead to a major contribution to the forces on the cylinder.

A lot of research[12, 13, 14, 15] has been conducted on LERC (leading edge rotating cylinder) utilizing the Magnus effect to act as a moving surface boundary layer control. Abdus's paper[15] shows the effect of Magnus effect created by the LERC. At all rotational velocities of the cylinder, the maximum lift coefficient increases with

rpm. This is driven by delay in flow separation and Magnus effect. This shows how a LE cylinder can be used as a MSBC to enhance aerodynamic effects. However, there are a lot of factors that contribute to different results for using LERC on an airfoil. Yuan Zhang[11] studies the different parameters that are required to optimize the design of leading edge rotating cylinders. The airfoil profile tested in his study is shown in figure and the proposed design for a better LERC is also shown in figure 1. Both these designs contain the similar LERC but differ in airfoil geometry.

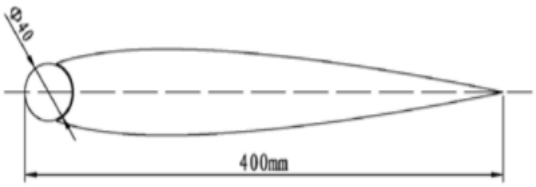

Fig 1. LERC design by Yuan Zhang[11]

Figure 1 shows a suggested design for a rotating cylinder on the leading edge of the airfoil. The given configuration was tested experimentally by Yuan Zhang and found out that it generates lift even at zero degree angle of attack, which was exceptional for a symmetric airfoil. Further, the designs were changed and improved by considering a non-symmetric airfoil with a larger camber, as shown below.

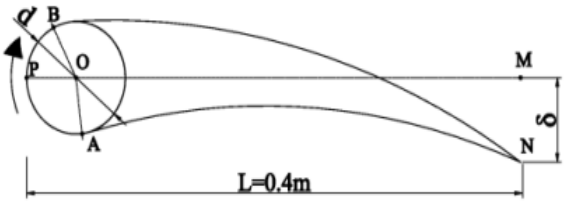

Fig 2. Improved configuration of Yuan's airfoil[11]

Given figure represents the better proposed airfoil that differs from the conventional airfoil by making the curve as smooth as it can over the airfoil. This will reduce any sudden break or angle in the flow which would lead to a delay in flow separation.

Below figure 3 shows the L/D ratio of original vs modified NACA 2412 airfoil. It concludes that even though at low angle of attacks the produce lift is less but figure 4 shows the increase in Cl of the airfoil. This trade off between L/D ratio and increase in coefficient of lift needs to be taken into consideration before coming to a conclusion about which airfoil to utilize. This study[16] also opens up various avenues of research where the rotating cylinder is placed at different points on the airfoil. The position of the rotating cylinder is dependent on where point of flow separation takes places and how the flow re-energization affects the flow.

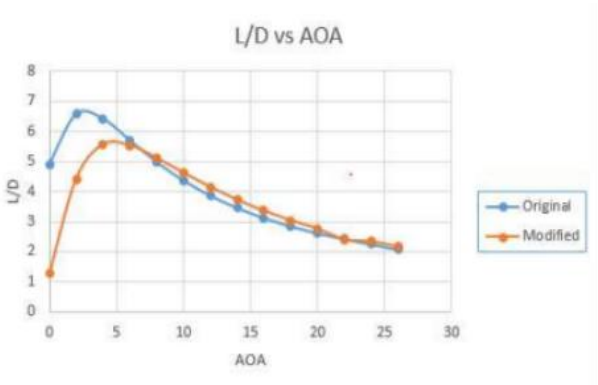

Fig 3. L/D vs AOA for original 2412 airfoil v/s modified 2412 airfoil [16]

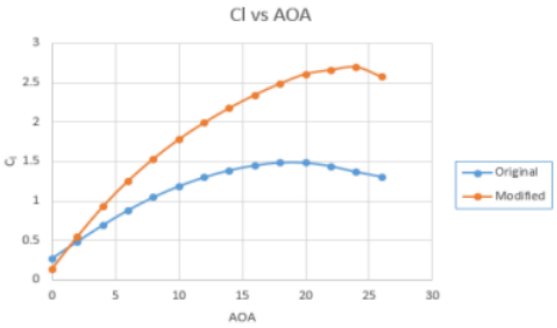

Fig 4. Cl vs AOA for original 2412 v/s modified 2412 airfoil [16]

The following graphs are a result of Vinayaka's[16] experiments where he modified a NACA 2412 airfoil and calculated its L/D ratio and C_l with respect to angle of attack (α)

A. Identification of problem

Modern day wings uses high lift devices such as flaps and slats which increases the efficiency of the wing during critical maneuvers such as take-off and landing. But this is performed on the cost of flow separation at an early chord length and increment of drag. If the flaps or slats are deployed incorrectly or if their aerodynamic performance is compromised, it can result in sudden and unpredictable stall behavior

B. Research Objective

The main objective of this paper is to create an aerodynamically efficient design of wing comprising rotating slots on leading edge and trailing edge. Also, to study the lift and drag values of rotating slots by using simulation techniques and to study the flow separation

and compare with conventional wing designs used in modern day aircrafts will give an insight on how useful the MSBC technology is as per the future requirements.

II. METHODOLOGY

The methodology used for the domains of this paper is a multistage process, which includes design and analysis of a base model, I.e. NACA 2412 geometry, and analysis of modified airfoil. The modified airfoil consist of LERC and TERC of known parameters(as designed in the design constrains) and rotates at a known angular acceleration (as discussed in the setup section). Further, each design has to undergo various step for computational simulation to give precise and reliable results. The steps for computational analysis are:

- Geometry creation
- Meshing
- Solver setup(Boundary condition)
- Post processing

After the following steps are followed, the results obtained are compared graphically. These graphs help in understanding the trends of variable parameters such as C_l and C_d.

A. Base Design

1) Geometry

The initial design for testing was taken to be of NACA 2412 airfoil. The main reason for choosing this airfoil was the widespread use of the airfoil in modern day aviation. If the modifications of design are successful for NACA 2412, then it opens a plethora of opportunities for MSBC to be applied in commercial aviation. The steps in designing the geometry included getting a CSV file for the co-ordinates of the said airfoil. Then using a CAD software to plot those lines into the actual shape of geometry. The co-ordinate file has been taken from the airfoil tools website[17].

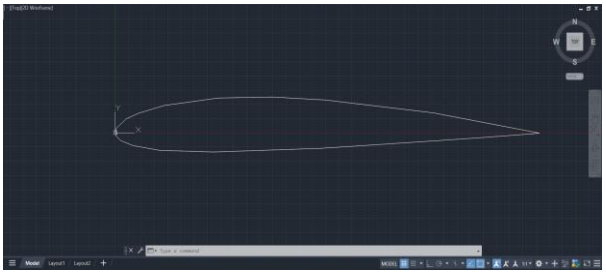

Fig 5. NACA 2412 geometry

The following figure shows basic geometry of NACA 2412 without any modifications to it. This geometry will help to validate our simulation results to previously known results.

The geometry was then imported to design modeler in order to create its fluid domain. For the given geometry, a C type domain was used to help study the fluid flow at various angles of attack. The c type domain helps meshing to be as refine and as efficient as possible.

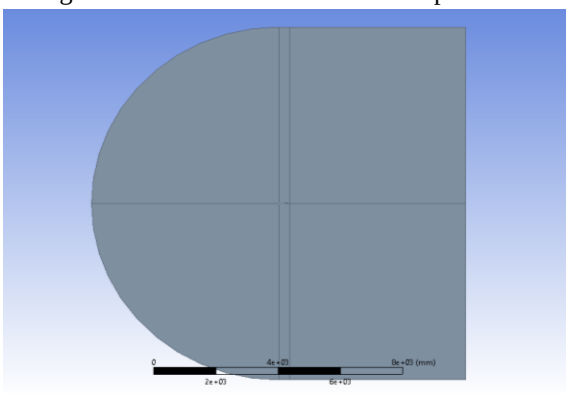

Fig 6. Fluid domain around the airfoil

2) Meshing

The mesh is most important part of any computational analysis. This is because all the calculations that happens in a simulation takes place at the nodes of the mesh. So finer the mesh, more accurate the simulation. For the given geometry, the domain was divided into 6 faces which were given individual properties of meshing to create a structures mesh. The mesh used for simulation was a quadrilateral dominant mesh, because it best fits the geometry and gives highly accurate results even with the limited computational power. Also, bias factor of 1000 was used in order to get a finer mesh near the airfoil body so that a result of higher accuracy could be obtained.

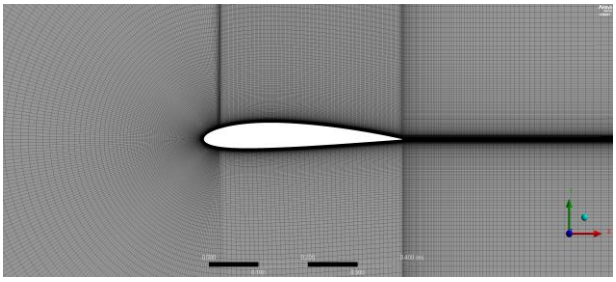

Fig 7. Meshing of NACA 2412

The figure above represents the mesh used for computational analysis of the base design, As it can be observed, the mesh is finer around the body and behind the trailing edge. This represents the areas, where high accuracy of the simulation is required.

Mesh Quality: Quality metrics for the mesh are rigorously adhered to, ensuring that the minimum orthogonal quality remains around 7.8 x 10-1. Aspect ratios are controlled to maximize resolution without

compromising computational efficiency—typically not exceeding 3.4 in areas around the fins. These parameters are crucial for reducing numerical diffusion and improving the accuracy of the simulation results.

B. Modified Design

1) Geometry

The geometry modification in NACA 2412 is based on the research done by Vinayaka's paper[16], where a rotating cylinder with radius of 5 % of the chord length at leading edge and similar cylinder with radius 2.5 % of the chord length at the trailing edges are employed. Also, for the passage of re-energized air, a slit of width 0.5 % of the chord length is provided.

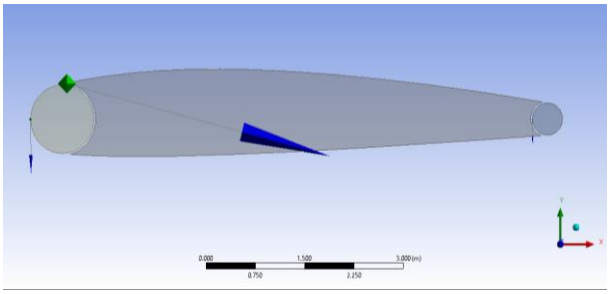

Fig 8. Modified airfoil geometry with LERC and TERC

The figure shows how the geometry is being modified by addition of rotating cylinders on the leading edge and trailing edge. The cylinders are free to rotate in specified directions with an angular velocity ω, such that ω/U∞>1, where U∞ is free stream velocity.

2) Meshing

As discussed earlier, meshing for the given geometry is a complex process, involving the need of finer mesh at the interface near the bodies. The mesh for the given geometry needs to be quadrilateral as well as structured in nature in order to provide the highest accuracy. Quadrilateral mesh is being used because it is easier to structure and provide highest accuracy at comparatively lower computational cost. Once again, biasing of the mesh with bias factor of 1000 provides a finer mesh at the airfoil body as compared to the outer domain.

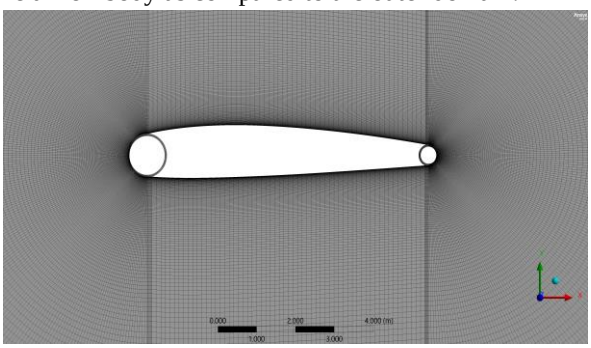

Fig 9. Meshing of modified geometry

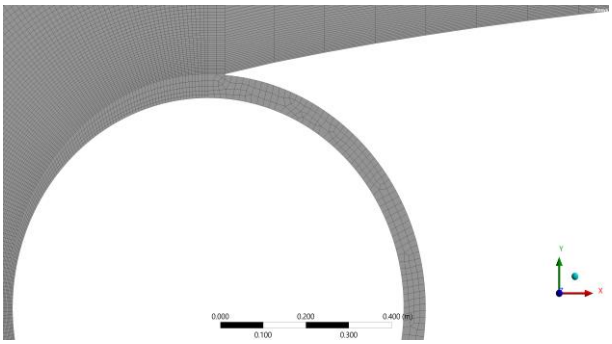

Fig 10. Meshing of slit between body and cylinder

Mesh Independence Study: To make our simulation independent of element size, a series of grid refinements are made and the number of elements are increased from 40,000 to 2,00,000. It is observed that the simulation results become independent of element size when the number of elements exceeds 90,000. Hence, the number of elements chosen for the mesh for this simulation is 95,000.

C. Solver Setup

The boundary condition is to given to simulate a real life environment faced by an airplane while multiple phases of a flight. The boundary conditions are taken as reference from Yuan Zhang's experimental setup[11].

- Pressure based solver
- Free stream velocity: 20m/s
- Density: Ideal Gas
- Temperature: 300 K
- Angle of attack, α: 0° to 15°
- Solver: Coupled

The simulation employs a solver setup configured for second-order accuracy, crucial for capturing the fine-scale phenomena critical to understanding aerodynamics over an airfoil and between the fine slits. The second order in this case refers to the fact that solver solves up to two terms of Taylor series expansion.

This expanded methodology provides a comprehensive framework for the CFD analysis of modified airfoil geometry, enabling us to thoroughly assess the impact of geometric alterations on aerodynamic properties. By leveraging precise geometry modeling, meticulous meshing, and sophisticated boundary condition setups, our study aims to optimize re-entry vehicle design.

D. Turbulence Model

RANS Single-Equation Model: Spalart-Allmaras [18]

A one-equation turbulence model called Spalart-Allmaras (SA) was created especially for aerodynamic flows such trans-sonic flow over airfoils. Kinematic eddy viscosity and mixing length serve as the

model's foundation. The turbulent viscosity's transport is determined by this mixing length. The resilience and quick implementation of the model for modeling specialized flows are major contributing factors to its popularity. Spalart-Allmaras has strong convergence and requires little memory.

A damping function in the Spalart-Allmaras model successfully manages near-wall flows, when turbulence effects are severe. With the use of this feature, the model can more accurately anticipate wall-bounded flows, like boundary layers and wall jets, without needing to adjust the grid too close to walls.

The transport equation used by the model is as follows:

$$\frac{\partial}{\partial t}(\tilde{\nu}) + \mathbf{U}\cdot\nabla(\tilde{\nu}) = c_{b1}S\tilde{\nu} - c_{w1}\left(\frac{\tilde{\nu}}{d}\right)^2 + \frac{1}{\sigma}\left[\nabla\cdot((\nu+\tilde{\nu})\nabla\tilde{\nu}) + c_{b2}(\nabla\tilde{\nu})\right.$$

Where,

- t is time
- U is velocity vector
- S is magnitude of strain rate tensor
- d is distance to nearest wall
- ν is molecular viscosity
- c_{b1}, c_{w1}, and c_{b2} are model constants
- F is additional terms for specific flow conditions

III. Result and Discussion

The computational analysis of base geometry and modified geometry has yielded fruitful results. The results of base geometry are similar to that of the reference papers[19, 20], which validated the computational analysis for the modified geometry. The extensive study gives result for coefficient of lift and drag for base and modified design, along with contours for pressure and velocity.

A. Base Design

The results from analysis of base design (NACA 2412) has helped us to validate our simulations. With the results with less than 5% error values, we can safely continue with our analysis for the modified design. The results from analysis of the base design are as follows:

1) Coefficient of lift

The coefficient of lift varies almost linearly with the angle of attack(α) until stall angle, which in this study was found to be 15°. Beyond the stall angle, the lift starts to reduce rapidly and drag becomes very high. The variation of C_l with α is as follows:

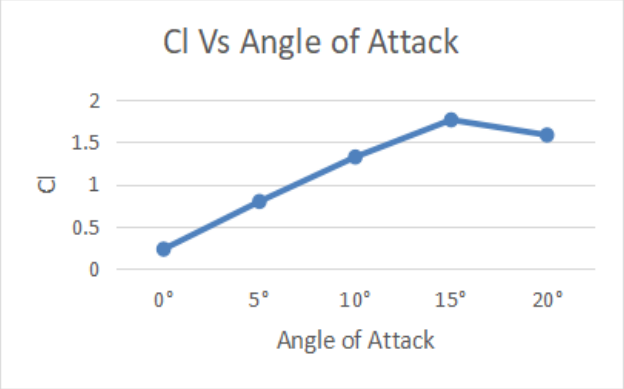

Fig 11. C_l vs A.O.A. for NACA 2412

2) Coefficient of drag

The coefficient of drag varies as a parabolic curve with the angle of attack(α) until 10°. Beyond the 10° angle, the drag starts to increase rapidly and drag becomes very high. The variation of C_d with α is as follows:

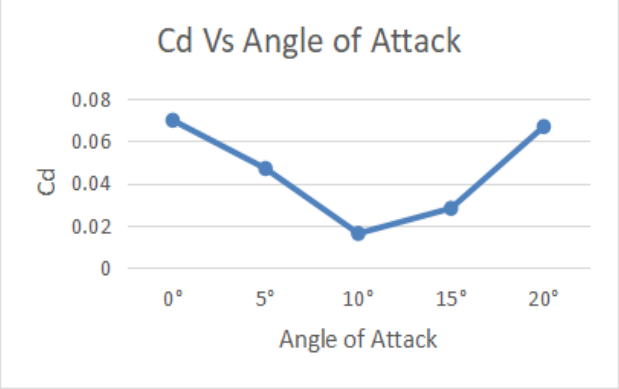

Fig 12. C_d vs A.O.A. for NACA 2412

3) Pressure and Velocity contours

In every contour, the pressure and velocity tends to follow a trend, where pressure always tends to be lower on the top surface of the airfoil and higher on the bottom. The velocity followed an opposite trend to that of pressure. For velocity, maximum value was achieved at the top surface of the airfoil and minimum at the bottom one. The contours of velocity and pressure at various angles of attack can be observed below from figure to figure.

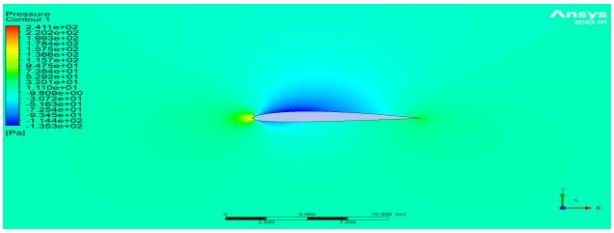

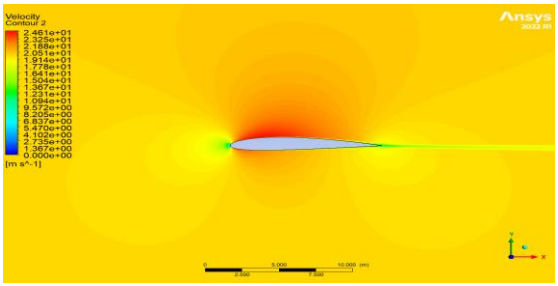

Fig 13. Contours for NACA 2412 at 0° A.O.A
(i) Pressure Contour(Left)
(ii) Velocity Contour(Right)

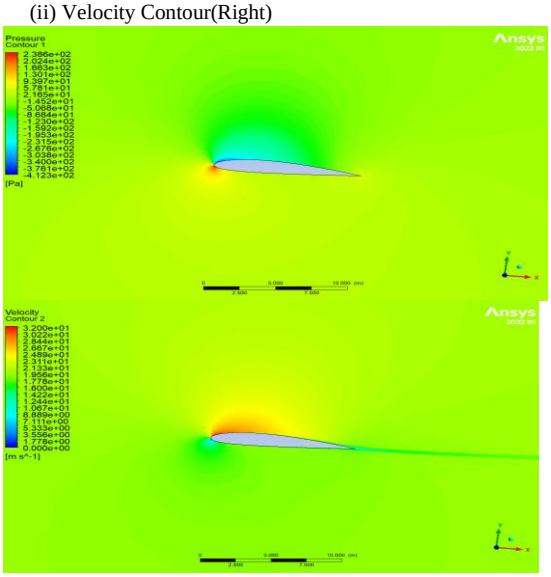

Fig 14. Contours for NACA 2412 at 5° A.O.A
(i) Pressure Contour(Left)
(ii) Velocity Contour(Right)

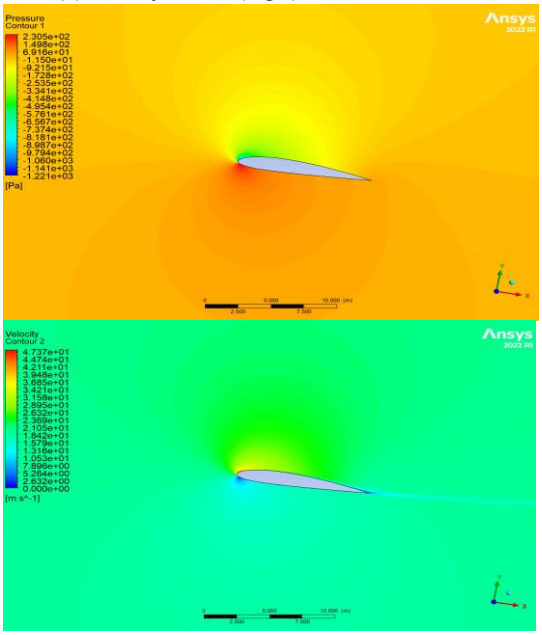

Fig 15. Contours for NACA 2412 at 10° A.O.A
(i) Pressure Contour(Left)
(ii) Velocity Contour(Right)

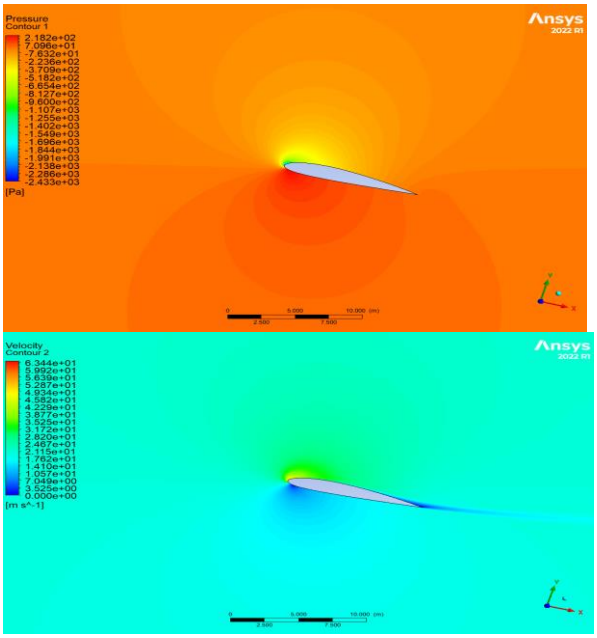

Fig 17. Contours for NACA 2412 at 15° A.O.A
(i) Pressure Contour(Left)
(ii) Velocity Contour(Right)

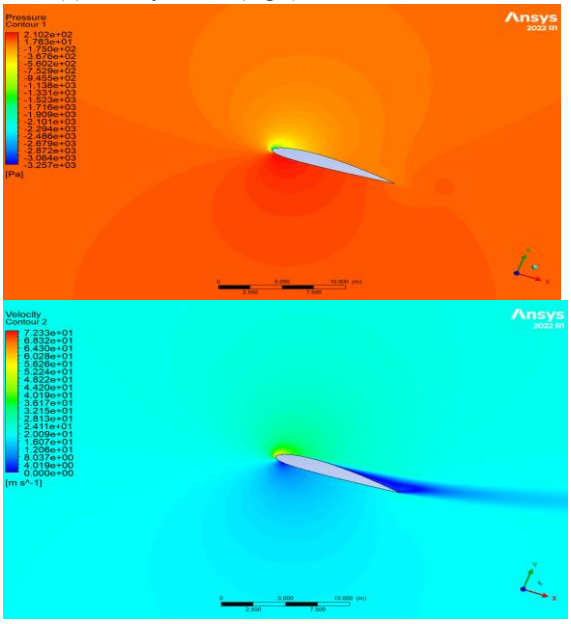

Fig 18. Contours for NACA 2412 at 20° A.O.A
(i) Pressure Contour(Left)
(ii) Velocity Contour(Right)

B. Modified Geometry

The simulation of geometry where LERC and TERC are applied, successfully gives an improved version of the airfoil, by increasing the lift coefficient and reducing the drag coefficient. After setup, the simulation was run by giving an angular velocity of 125 rad/sec to the LERC and 250 rad/sec to the TERC. After the given setup, following results were yielded:

1) Coefficient of lift

The coefficient of lift was found to be increased for every angle of attack variation, which itself results the airfoil to be an aerodynamically better design. Further, the stall angle seems to be increased from 15° to some value greater than 20°. This change was observed because even at 20° angle of attack, the lift coefficient was showing a rise in its value and stall had not occurred. The variation of C_l with angle of attack can be observed in figure.

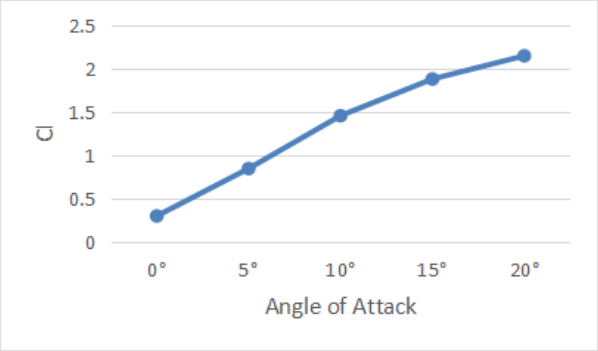

Fig 19. C_l vs A.O.A. for airfoil with LERC and TERC

2) Coefficient of Drag

Similar to the NACA 2412, modified geometry also follows a parabolic curve to define coefficient of drag at various angles of attack. The drag decreases up to 10° angle of attack and increases rapidly afterwards. The variation of C_d with α is as follows:

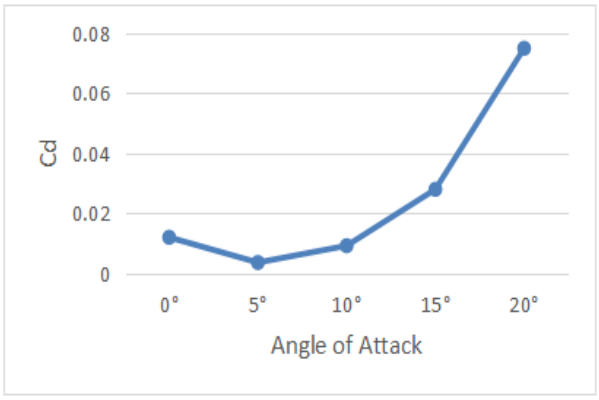

Fig 20. C_d vs A.O.A. for airfoil with LERC and TERC

3) Pressure and Velocity contours

Contours of pressure and velocity shows a very important feature of the geometry. It can be clearly observed in the contours that the air is seeping into the given slit. Hence, energizing the flow which results in the implementation of Magnus effect. Also, a trend similar to velocity and pressure contour of base design can be seen where pressure is higher at the lower surface of the airfoil and vice versa in case of velocity. The contours of pressure and velocity for modified geometry are given below

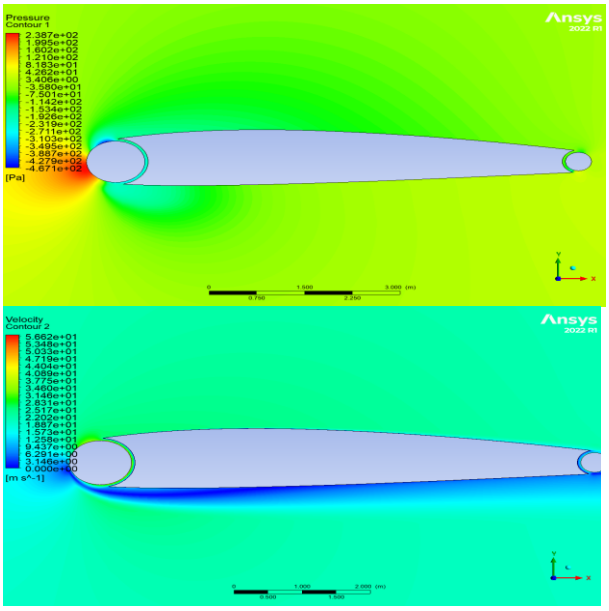

Fig 21. Contours for LERC and TERC at 0° A.O.A
(i) Pressure Contour(Left)
(ii) Velocity Contour(Right)

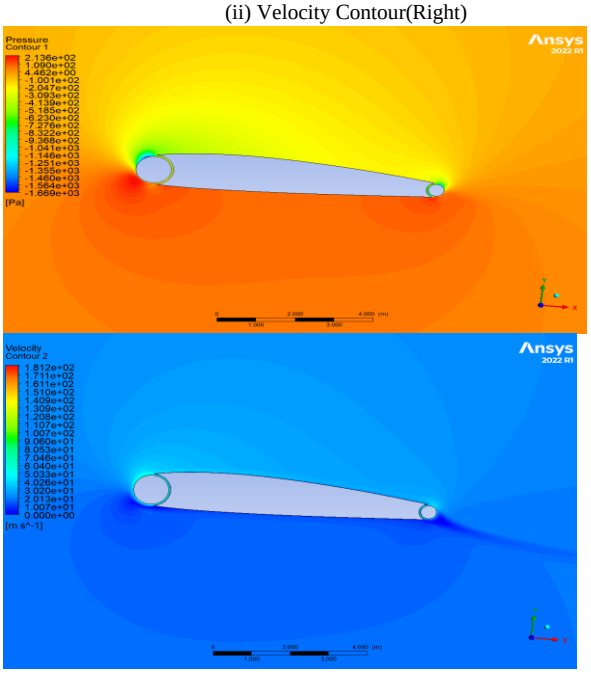

Fig 22. Contours for LERC and TERC at 5° A.O.A
(i) Pressure Contour(Left)
(ii) Velocity Contour(Right)

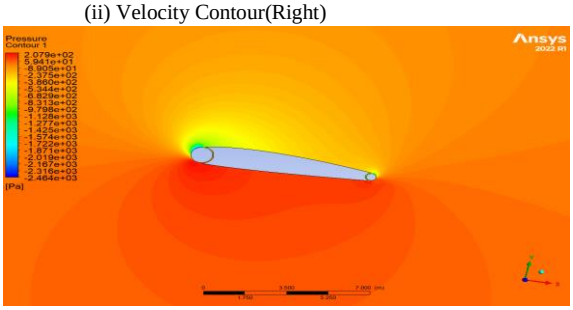

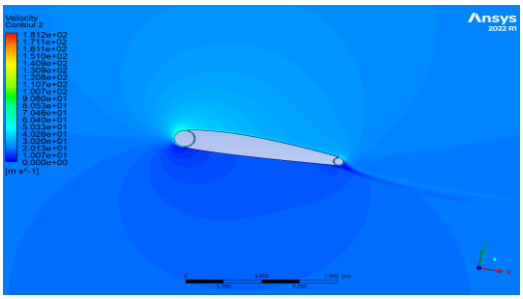

Fig 23. Contours for LERC and TERC at 10° A.O.A
(i) Pressure Contour(Left)
(ii) Velocity Contour(Right)

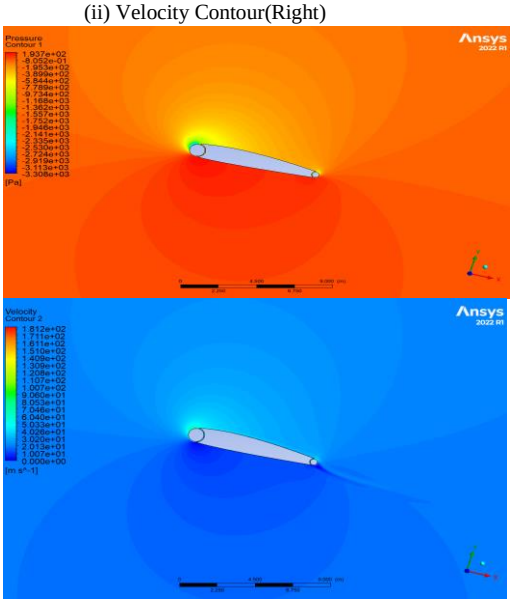

Fig 24. Contours for LERC and TERC at 15° A.O.A
(i) Pressure Contour(Left)
(ii) Velocity Contour(Right)

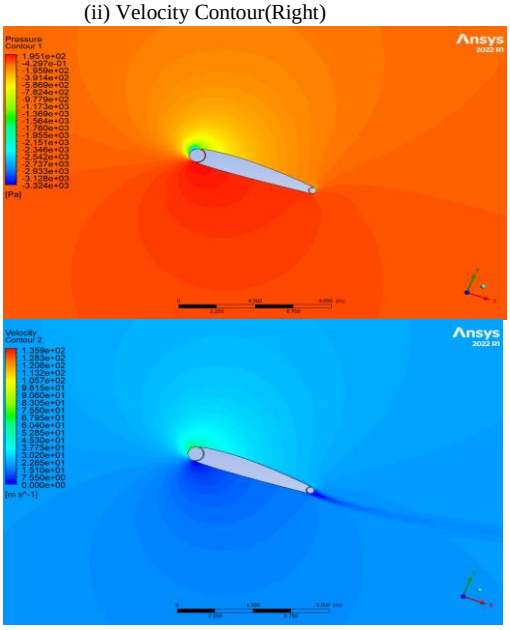

Fig 25. Contours for LERC and TERC at 20° A.O.A
(i) Pressure Contour(Left)
(ii) Velocity Contour(Right)

C. Graphical Comparison.

Gathered results are plotted into a graphical form to obtain a better understanding and effectiveness of the modification. The trend lines of graph clearly represents that the change in the geometry has given promising results by increasing the overall lift coefficient of the airfoil, as well as reducing the drag coefficient at certain angles of attack. Another observation that can be made from the graph is that the coefficient of lift does not fall dramatically after the stall angle is reached (observed to be 15° for NACA 2412). The graphical comparisons for coefficient of lift and drag are given below in figure and figure.

Table 1. Cl vs Angle of Attack comparison for both geometries

C_l vs Angle of Attack					
Geometry\A.O.A	0	5	10	15	20
NACA 2412	0.225	0.793	1.324	1.767	1.586
LERC and TERC	0.296	0.844	1.455	1.879	2.147

Table 2. Cd vs Angle of Attack comparison for both geometries

C_d vs Angle of Attack					
Geometry\A.O.A	0°	5°	10°	15°	20°
NACA 2412	0.026	0.015	0.016	0.028	0.067
LERC and TERC	0.012	0.003	0.009	0.028	0.075

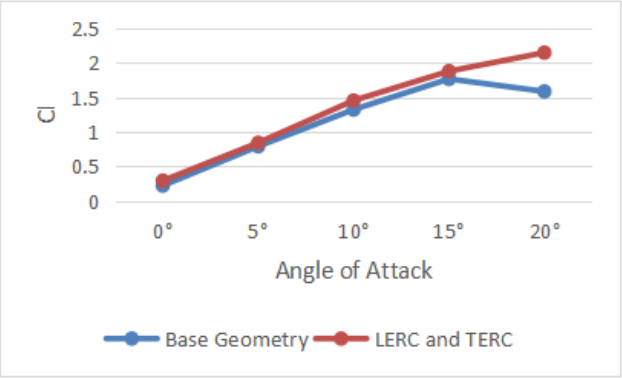

Fig 26. Comparison between C_l vs A.O.A. for NACA 2412 and geometry with LERC and TERC

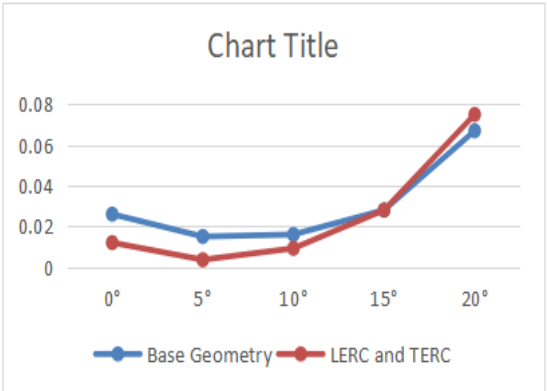

Fig 27. Comparison between C_l vs A.O.A. for NACA 2412 and geometry with LERC and TERC

IV. CONCLUSION

The CFD analysis of the modified airfoil geometry has revealed that the integration of rotating cylinders on leading and trailing edges, can positively influence the vehicle's ability to generate lifting force and reduce drag. The variations in coefficient of lift and coefficient of drag with angle of attack are indicative of the complex interplay between the vehicle's geometry and its aerodynamic environment. These findings provide a solid foundation for optimizing the design of the airfoil to enhance its performance and reduce structural complexity. The paper also confirms the relation between free stream velocity and angular velocity of rotating cylinders, $\omega/U\infty>1$[11].

REFERENCES

[1] John D. Anderson; Ludwig Prandtl's Boundary Layer. Physics Today 1 December 2005; 58 (12): 42–48.

[2] Modi, V. J. "Moving surface boundary-layer control: a review." Journal of fluids and structures 11.6 (1997): 627-663.

[3] Modi, V. J., et al. "High-performance airfoil with moving surface boundary-layer control." Journal of Aircraft 35.4 (1998): 544-553.

[4] Modi, V. J., et al. "Moving surface boundary-layer control as applied to two-dimensional airfoils." Journal of Aircraft 28.2 (1991): 104-112.

[5] Mittal, Sanjay, and Bhaskar Kumar. "Flow past a rotating cylinder." Journal of fluid mechanics 476 (2003): 303-334.

[6] Seifert, Jost. "A review of the Magnus effect in aeronautics." Progress in aerospace sciences 55 (2012): 17-45.

[7] Govardhan, D., et al. "Conceptual wing design blended with Magnus effect." Materials Today: Proceedings (2023).

[8] Ketan, S., et al. "Magnus effect on Aerodynamic Characteristics on Wing Airfoil MH45." International Journal of COMADEM 21.1 (2018).

[9] Lefebvre, Jonathan N., and Anya R. Jones. "Experimental investigation of airfoil performance in the wake of a circular cylinder." AIAA Journal 57.7 (2019): 2808-2818.

[10] Zhang, H. J., L. Huang, and Y. Zhou. "Aerodynamic loading on a cylinder behind an airfoil." Experiments in fluids 38 (2005): 588-593.

[11] Zhang, Yuan-yuan, et al. "Exploration in optimal design of an airfoil with a leading edge rotating cylinder." Journal of Thermal Science 19 (2010): 318-325.

[12] Du, X., et al. "Flow past an airfoil with a leading-edge rotation cylinder." Journal of aircraft 39.6 (2002): 1079-1084.

[13] Al-Garni, Ahmed Z., et al. "Flow control for an airfoil with leading-edge rotation: an experimental study." Journal of Aircraft 37.4 (2000): 617-622.

[14] Salam, Md Abdus, et al. "Numerical analysis of effect of leading-edge rotating cylinder on NACA0021 symmetric airfoil." European Journal of Engineering and Technology Research 4.7 (2019): 11-17.

[15] Salam, Md Abdus, et al. "Moving surface boundary layer control analysis and the influence of the Magnus effect on an aerofoil with a leading-edge rotating cylinder." (2019).

[16] Vinayaka, D. M., and Jamehdar Kouser Mubeena. "Effect of freely rotating cylinder mounted near the trailing edge of the wing for boundary layer separation delay." International Research Journal of Engineering and Technology (IRJET) 5.9 (2018): 255-261.

[17] http://airfoiltools.com/airfoil/details?airfoil=naca2412-il

[18] Spalart, Philippe, and Steven Allmaras. "A one-equation turbulence model for aerodynamic flows." 30th aerospace sciences meeting and exhibit. 1992.

[19] Kharulaman, Liyana, et al. "Research onFlows for NACA 2412 Airfoil using computational fluid dynamics method." Int. J. Eng. Adv. Technol 9.1 (2019): 5450-5456.

[20] Saxena, Er Shivam, and Mr Rahul Kumar. "Design of NACA 2412 and its Analysis at Different Angle of Attacks, Reynolds Numbers, and a wind tunnel test." International Journal of Engineering Research and General Science 3.2 (2015): 193-200.